Analysis of Relative Intensity Noise Spectra for Uniformly and Chirpily Stacked InAs–InGaAs–GaAs Quantum Dot Lasers

Gray Lin, *Member, IEEE*, Hao-Ling Tang, Hsu-Chieh Cheng, and Hung-Lin Chen

***Abstract*—The dynamic properties of uniformly and chirpily stacked InAs–InGaAs–GaAs quantum dot lasers are analyzed in terms of relative intensity noise spectra. For uniformly stacked quantum dot laser with ground-state lasing emissions of 1.3 μm, the K-factor limited bandwidth is 13 GHz. The extracted differential gain and gain compression factor are 1.7×10^{-15} cm^2 and 2×10^{-16} cm^3, respectively. For chirpily stacked quantum dot laser with excited-state lasing emissions of 1.2 μm, the K-factor limited bandwidth is 14 GHz. Yet the nonproportional dependence between resonance frequency and square root of incremental current yields differential gain of 4.3×10^{-15} cm^2 and huge gain compression factor of 1.4×10^{-14} cm^3.**

***Index Terms*—Differential gain, gain compression, relative intensity noise (RIN), quantum dot lasers.**

I. Introduction

IDEAL quantum-structure lasers with reduced dimensionality are expected to have the advantages of large material and differential gain, small frequency chirping, high temperature stability, as well as low threshold current. Therefore, quantum dot (QD) lasers, in particular GaAs-based 1.3-μm wavelength range, are attractive as next-generation light sources in the metro/access optical fiber communication networks. However, formation of nonideal QD by self-assembled approach suffers from limited dot density and large inhomogeneous broadening, which result in broad gain spectrum but rather low peak gain. It then deteriorates the modulation characteristics of QD lasers. The current solution to overcome these disadvantages is through multilayer stacking of QD.

To improve and investigate the modulation bandwidth of QD lasers, strategies are proposed and several successes are achieved. Their modulation characteristics are mostly studied by radio-frequency small-signal modulation (SSM) response [1]–[5]. For example, direct 10 Gb/s modulation of 1.3 μm QD lasers was first demonstrated in modulation p-doped structure, the 3 dB bandwidth is 7.7 GHz, and the K-factor limited bandwidth is over 10 GHz [1]. Another example, for ground-state (GS) emission QD lasers with tunneling injection structure, the measured 3 dB bandwidth was 11 and 24.5 GHz for p-doped samples of 1.3 and 1.1 μm range, respectively [2].

The limited saturation gain of QD GS results in excited-state (ES) or two-state lasing emissions in short-cavity devices or under high current injection. Previous investigation of ES-QD lasers to increase the modulation bandwidth is based on the two advantageous factors [3]. First, there is two/threefold degeneracy, or equivalently twice to triple the saturation gain, of the ES compared to the GS. Second, there should be decreased capture time from the carrier reservoir into the ES compared to the GS. Recently, high-speed direct-modulated ES emission QD lasers have been proposed and demonstrated by the University of Sheffield [3]. For ES lasing emissions of 1.19 μm, the measured 3 dB bandwidth was only 4.1 GHz due to RC parasitics. The predicted K-factor limited bandwidth for ES lasing emissions was 13 GHz.

Another method to evaluate the direct modulation capabilities is by relative intensity noise (RIN) measurement, which is parasitic-free. The RIN measurements of QD laser were scattered in recent publications, however, analysis of RIN spectra can rarely be found. This is attributed to the highly damped modulation response that leads to very low RIN levels which are critical in the measurement. First RIN measurement of GS QD lasers was presented in [6] and [7]. No resonance peak was observed in these long-cavity (>2.5 mm) devices. The completely damped response provides an RIN level of -159 dB/Hz, which is flat within ± 2 dB/Hz in 0.1–10 GHz range. The RIN spectra of GS-QD lasers with clear and distinct peak were presented by Capua *et al.* [8]. The resonance peak was around 3 GHz at 1.7 mW for 1 mm device; nonetheless, the periodic oscillations at high frequencies keep them from further analysis. First RIN analysis of GS QD lasers was presented by Martinez *et al.* [9]. The InAs–InP QD lasers grown on a specific InP (3 1 1)B substrate are emitting at 1.52 μm. Its clear resonance peak at maximum of 3.8 GHz from 1.1 mm device indicated less damping than InAs–GaAs QD lasers.

In this paper, the RIN spectra of uniformly and chirpily stacked QD lasers are measured for GS and ES lasing emissions, respectively. The dynamic properties of modulation bandwidth, resonance frequency, and damping coefficient are resolved by fitting the theoretical RIN expression. The device parameters of differential gain and gain compression factor are, therefore, extracted. The estimated maximum 3 dB bandwidths

Manuscript received August 08, 2011; revised October 03, 2011, December 01, 2011; accepted December 09, 2011. Date of publication December 15, 2011; date of current version January 27, 2012. This work was supported by the Ministry of Education under the Aiming for the Top University and Elite Research Center Development Plan as well as the National Science Council Project under Contract NSC 99-2221-E-009-176.

The authors are with the Department of Electronic Engineering and Institute of Electronics, National Chiao-Tung University, Hsinchu 30010, Taiwan (e-mail: graylin@mail.nctu.edu.tw; to_chris827@hotmail.com; u890851@alumni.nthu.edu.tw; hakuoro0301@gmail.com).

Color versions of one or more of the figures in this paper are available online at http://ieeexplore.ieee.org.

Digital Object Identifier 10.1109/JLT.2011.2179974

as well as the device parameters are consistent with those from SSM analysis [2], [3]. Yet the linear, instead of proportional, dependence of resonance frequency versus square root of incremental current is observed and discussed for chirpily stacked QD lasers.

II. Theory and Experiment

A. Dynamic Analysis

The modulation characteristics and noise spectra are governed by the same dynamical processes, and we have assumed that single-longitudinal mode rate equations for photon and carrier can provide a sufficiently good description for the dynamics of QD lasers around resonance frequency. The derived expression for RIN spectra is given by [10]–[12]

$$\mathrm{RIN}(f) = \frac{4}{\pi}\delta f_{\mathrm{ST}} \frac{f^2 + (\xi/2\pi)^2}{\left(f^2 - f_r^2\right)^2 + f^2(\gamma/2\pi)^2} \tag{1}$$

with

$$\gamma = K f_r^2 + 1/\tau_{\mathrm{eff}} \tag{2}$$

$$f_r \approx D\sqrt{P} = \mathrm{MCEF}\sqrt{J - J_{\mathrm{th}}}. \tag{3}$$

In (1), δf_{ST} is the Schawlow–Townes linewidth, f_r is the resonance frequency, γ is the damping coefficient, while ξ in the numerator is the exact damping factor including the nonlinear gain [11]. τ_{eff} in (2) is the spontaneous emission carrier lifetime. P and J_{th} in (3) are light output power and threshold current density, respectively. Note that (3) is approximately valid at low current injection.

The K-factor, D-factor and modulation current efficiency factor (MCEF) are introduced for convenience, where differential gain and maximum modulation bandwidth could then be extracted within. They are given by

$$K = \frac{(2\pi)^2}{v_g}\left(v_g \tau_{\mathrm{ph}} + \frac{\varepsilon}{dg/dn}\right) \tag{4}$$

$$D = \frac{1}{2\pi}\left[2\left(\frac{\Gamma}{V_a}\right)\frac{v_g dg/dn}{h\nu}\left(\frac{\alpha_i + \alpha_m}{\alpha_m}\right)\right]^{1/2} \tag{5}$$

$$\mathrm{MCEF} = D\sqrt{\left(\frac{dP}{dI}\right) L \times W}. \tag{6}$$

In (4), v_g is the group velocity, τ_{ph} is the cavity photon lifetime, ε is the nonlinear gain coefficient, and dg/dn is the differential gain. In (5), Γ is the optical confinement factor, V_a is the active volume, $h\nu$ is the photon energy, and α_i and α_m are the internal and mirror losses, respectively. In (6), dP/dI is the slope efficiency of L–I curve, and L and W are the cavity length and waveguide width, respectively.

B. Transport Effect

To describe the carrier transport between multilayer structure and carrier relaxation within multiple energy states, several comprehensive models were proposed but most of them concerned about SSM response [12]–[18]. The RIN measurement, which is independent of transport and parasitic effects, depends only on intrinsic dynamics of active region. Therefore, the additional first-order pole present in the SSM response is absent in the RIN expression [12], [13].

The equivalent modification is by introducing the transport factor in the differential gain in (4) and (5), i.e., the effective differential gain is redefined by division of transport factor ($\chi = 1 + \tau_{\mathrm{c}}/\tau_{\mathrm{esc}}$), where τ_{c} is the transport time which include capture, and τ_{esc} is the carrier escape time [12], [15]. Since the definition of time constant varies in different models and the values spread in a large range [17], [18], the transport factor is rarely discussed in publications [13], [15]. Therefore, it is the effective differential gain which inclusive of the transport division factor that we have meant in this study.

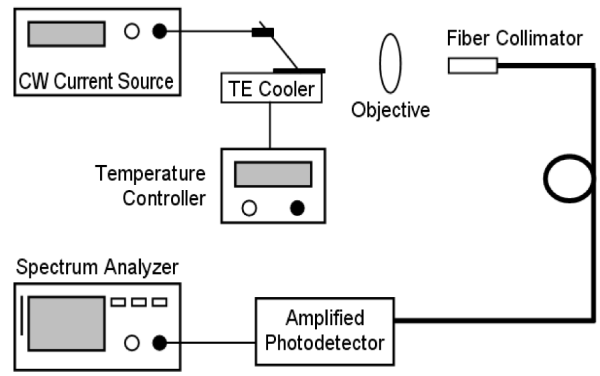

Fig. 1. Experimental setup for RIN measurement of QD lasers.

C. Measurement Setup

Fig. 1 shows the experimental setup for RIN measurement. The measurement is performed under continuous-wave (CW) current injection with temperature controlled by thermoelectric cooler. The optical signals are fiber-coupled to an amplified photodetector (Newport AD-10ir) followed by an electrical spectrum analyzer (Agilent E4407B). To lower the optical feedback, the light output power is first attenuated, slightly tilted off-axis, and collimated by a microscope objective. It should be noted that the thermal noise of measurement system and the shot noise of amplified photodetector are subtracted in correcting the measured spectra [8]. Because of the unique low RIN levels of QD lasers, the suggested cavity lengths are not longer than 2 mm in case resonance characteristics are damped or averaged out by multilongitudinal modes.

D. Laser Structures

Two QD laser structures are grown by molecular beam epitaxy on (1 0 0) oriented Si-doped GaAs substrates. Fig. 2 shows the schematic active regions for uniformly and chirpily stacked QD laser structures. The QDs are self-assembled using Stranski–Krastanov growth method. Both active regions consist of InAs QD capped by InGaAs QW.

For uniformly stacked structure, the capped InGaAs QW are kept at the same thickness and the GS lasing wavelength is around 1.3 μm. The single-layer dot density is about 6×10^{10} cm^{-2} and eight-layer QD stacks with p-doped GaAs spacer are grown to increase the optical gain.

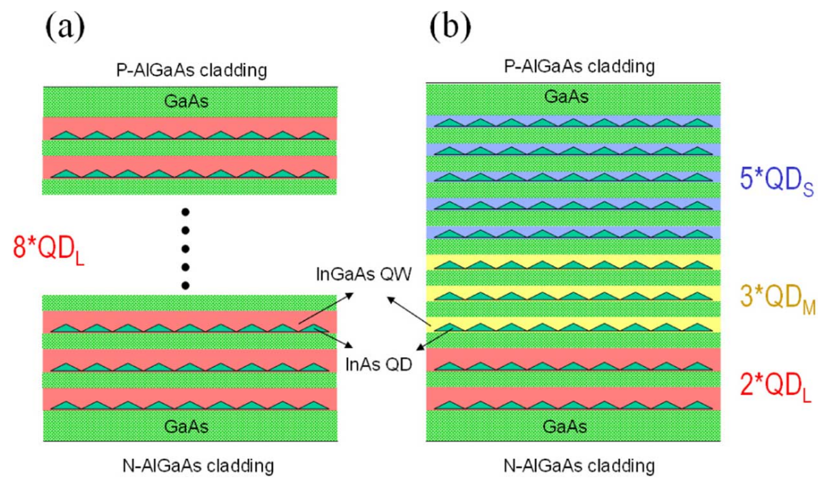

Fig. 2. Schematic active regions for (a) uniformly and (b) chirpily stacked QD laser structures.

For chirpily stacked structure, the capped InGaAs QW of 4, 3, and 1 nm are designed for three chirped wavelengths of longer, medium, and shorter wavelength range, with stacking numbers of 2, 3, and 5 layers, respectively, and designated as $2^*\mathrm{QD_L}$, $3^*\mathrm{QD_M}$, and $5^*\mathrm{QD_S}$ [19]. The GS/ES wavelengths are in wavelength ranges of 1.27/1.19, 1.22/1.15, and 1.17/1.10 μm for longer, medium, and shorter wavelength QD stacks, respectively. The detailed layer structure and growth of QD can be found in [19].

The chirpily stacked QD lasers of 5 μm width are as-cleaved (CL/CL) and left unpackaged, while the uniform-stack QD lasers of 2 μm width and 300 μm length are coated with high-reflectivity on one side (HR/CL) and packaged in transmitter optical sub-assembly package.

III. Results and Discussion

A. DC Characteristics

Fig. 3 shows the CW light–current (L–I) and spectral characteristics of QD lasers. For uniformly stacked QD laser of 300 μm cavity in Fig. 3(a), the low threshold current of 8 mA (or 1333 A/cm^2) with superior temperature stability is shown and the lasing emission is in the GS of 1.3 μm range. While for chirpily stacked QD laser chip of 750 μm length in Fig. 3(b), the threshold current is around 33.3 mA (or 888 A/cm^2) and lasing emission is in 1.2 μm range. The slope efficiency of front-side light output is 0.5 and 0.28 W/A for uniformly and chirpily stacked QD lasers, respectively.

Due to the limited saturation gain of single-layer QDs, the lasing emissions switch between GS and GS and exhibit a sudden change of peak wavelength in the varying-cavity-length measurement of as-cleaved devices. For uniformly stacked eight-layer QD lasers, the maximum modal gain is over 40 cm^{-1} and no ES emissions were observed for cavity lengths over 300 μm. For chirpily stacked QD lasers, the peak wavelength shifted at cavity lengths of 2 and 0.5 mm, as shown in Fig. 6 of [19]. Based on analysis of dependence of threshold modal gain on current density, the lasing emissions for cavity below 2 mm switched from $\mathrm{GS}-2^*\mathrm{QD_L}$ to $\mathrm{GS}-3^*\mathrm{QD_M}$, while that below 0.5 mm switched from $\mathrm{ES}-2^*\mathrm{QD_L}$ to $\mathrm{ES}-5^*\mathrm{QD_S}$. The peak wavelength around 1.2 μm for 750 μm device is, then, identified as lasing emission from $\mathrm{ES}-2^*\mathrm{QD_L}$.

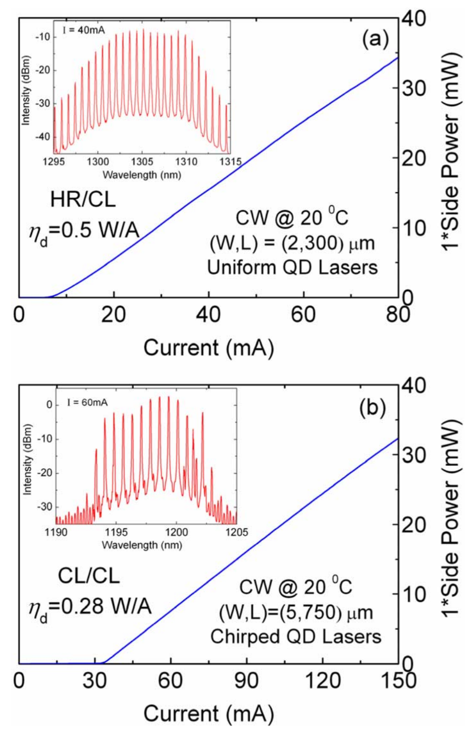

Fig. 3. L–I curves and lasing spectra measured at 20 °C for (a) uniformly and (b) chirpily stacked QD lasers.

B. RIN Spectra

The typical RIN spectra for uniformly and chirpily stacked multilayer QD lasers under different injection current levels are shown in Fig. 4. The noise floor is as low as -155 dB/Hz under high current injection. For cavity longer than 1.5 mm (not shown), the resonance characteristics are completely damped to a very low level below -160 dB/Hz. At lower frequencies below 1 GHz, we observe an enhancement of RIN levels, which is due to mode competition. While at higher frequency range, the resonant peaks are decreasing and moving to higher frequencies with increasing current injection.

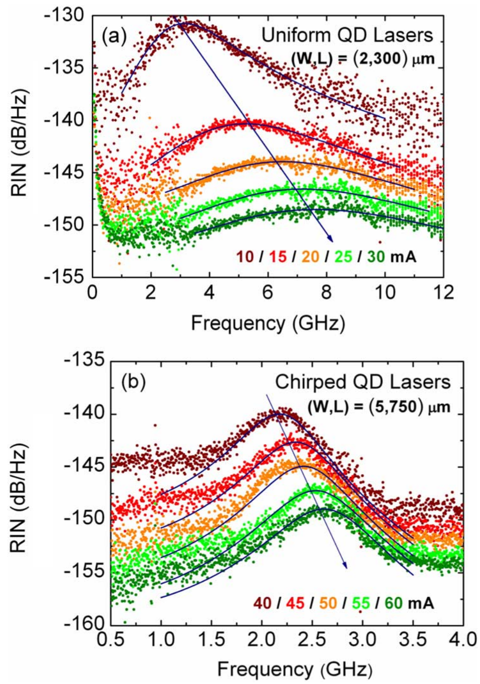

Fig. 4. RIN spectra for different injection current levels for (a) uniformly and (b) chirpily stacked QD lasers.

At first glance of Fig. 4(a) and (b), the uniformly stacked QD laser, with much reduced device dimension, experienced a faster shift of resonance frequency. To perform further analysis, these spectra are fitted to the expression in (1) around the peak resonance. The resonance frequencies as well as damping coefficients are, therefore, extracted.

C. K-Factor Limited Bandwidth

Fig. 5 shows the RIN analysis of intrinsic frequency response for QD lasers. Analysis of damping coefficient versus resonance frequency squared resolves the slope parameter of K-factor as defined in (2). The K-factor can be used to calculate the maximum K-factor limited bandwidth using

$$f_{3\,\mathrm{dB,max}} = \frac{2\sqrt{2}\pi}{K}. \tag{7}$$

For uniformly stacked QD laser in Fig. 5(a), the K-factor is 0.687 ns and the K-factor limited bandwidth is about 13 GHz, which puts the experimental limit of direct modulation for self-assembled QD lasers of GS lasing emission in 1.3 μm range. In comparison with some landmark results, the K-factor is 0.82 ns in p-doped QD lasers [1], [18] and at a rough estimate of 0.5–0.6 ns in p-doped tunnel-junction QD lasers of 1.3 μm range [2]. It is worth mentioning that the large K-factor of QD lasers, which is about 2–3 times the value of optimized InP-based multiple QW lasers [20], [21], is related to the highly damped frequency response and the rather lower limited modulation bandwidth [5].

For chirpily stacked QD laser in Fig. 5(b), the K-factor is 0.632 ns and the K-factor limited bandwidth is about 14 GHz. The K-factor limited bandwidth is close to the first SSM measurements of 15.2 GHz for ES uniformly stacked QD lasers [3]. However, it does not mean the predicted bandwidth is

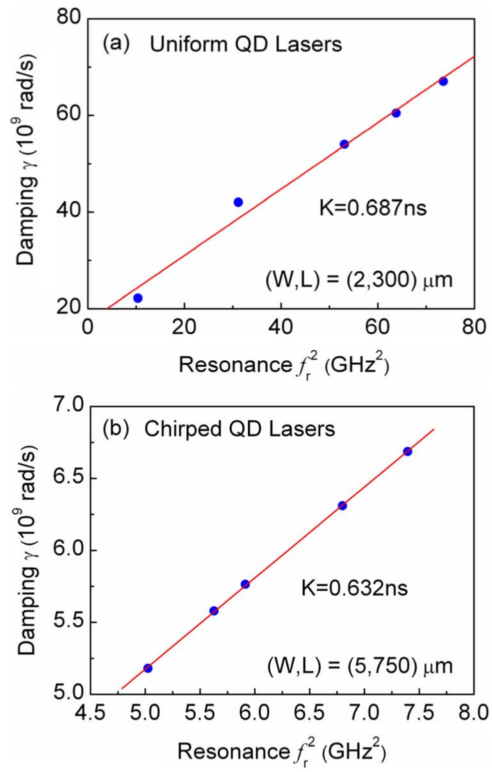

Fig. 5. Damping coefficient versus resonance frequency squared for (a) uniformly and (b) chirpily stacked QD lasers.

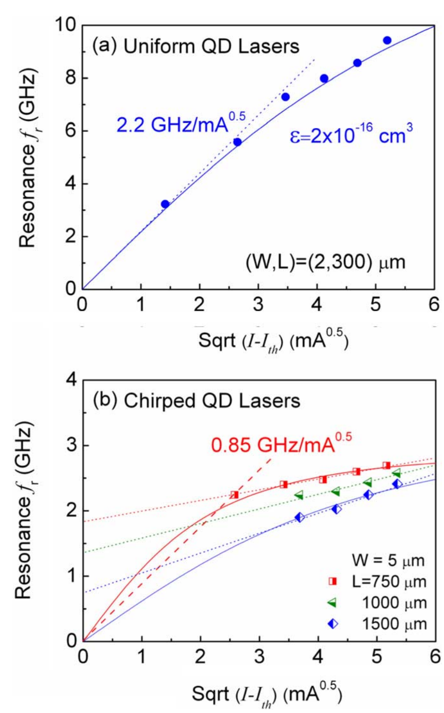

Fig. 6. Resonance frequency versus square root of incremental current for (a) uniformly and (b) chirpily stacked QD lasers.

practically achievable because it neglects self-heating and RC parasitics.

D. Differential Gain and Gain Compression Factor

The resonance frequency is plotted as function of square root of the incremental current in Fig. 6. For uniformly stacked QD laser in Fig. 6(a), it exhibits proportional dependence at low injection current (dotted line) as described in (3). The MCEF is 0.17 GHz/(A-cm^{-2})$^{0.5}$ (or 2.2 GHz/mA$^{0.5}$) under low injected current density of 1.3–3.3 kA/cm^2. By (3), (5), and (6), we extract the differential gain $dg/dn = 1.7 \times 10^{-15}$ cm^2, and the nonlinear gain compression factor $\varepsilon = 2 \times 10^{-16}$ cm^3 is calculated according to (4).

As the current injection is above three times the threshold (>3.3 kA/cm^2), the resonance frequency dependence on square root of current increment shows a decreased slope. This effect of gain saturation is first described and fitted in Fig. 3.20 of [22]. As a result, (3) should be modified according to the following expressions [21], [22]:

$$f_r = \frac{1}{2\pi}\sqrt{\frac{v_g}{\tau_{\rm ph}}\frac{dg}{dn}\frac{S}{1+\varepsilon \cdot S}} = \frac{D\sqrt{P}}{\sqrt{1+\varepsilon \cdot S}}. \quad (8)$$

The solid line in Fig. 6(a) is the fitting curve by substituting the extracted differential gain and nonlinear gain compression factor into (8). It is in good agreement with the experimental data points. By the way, the large nonlinear gain compression factor is one order-of-magnitude higher than the value of InP-based multiple QW lasers [20]–[23]. Since device heating is not observed in the measurement range, the reduced differential gain or the large gain compression is mainly attributed to the retarded carrier relaxation process in QD [23]–[25].

For chirpily stacked QD laser in Fig. 6(b), the proportionality constant is failed to be determined in the measurement range. Instead, one can observe a linear dependence. By directly connected each data point to the origin in Fig. 6(b), the MCEF values vary over a wide range. The maximum MCEF is estimated to be 0.16 GHz/(A-cm^{-2})$^{0.5}$ (or 0.85 GHz/mA$^{0.5}$) for 750 μm cavity. Using (3)–(6), we have corresponding values of $dg/dn = 2.1 \times 10^{-15}$ cm^2 and $\varepsilon = 1.9 \times 10^{-16}$ cm^3.

E. Discrepancy in Chirpily Stacked QD Lasers

The equivalent differential gain is a constant well-defined value when two-level rate equation system is used to describe the laser dynamic; however, it is not constant in QD semiconductor lasers with multipopulation energy levels as concluded in [16]. The decreasing differential gain or incomplete gain clamping above threshold is better described by the nonlinear gain compression factor.

If (10) is fitted to data points of 750 μm cavity, it renders $dg/dn = 4.3 \times 10^{-15}$ cm^2 with huge $\varepsilon = 1.4 \times 10^{-14}$ cm^3. This huge gain compression factor is not unreasonable because its order of magnitude is around the range from 5×10^{-15} to 1×10^{-16} cm^3 as predicted in [26]. The huge gain compression is attributed to excess carrier leakage associated with carriers populated in higher and broadened energy range. To put it differently, the intentional multiple electron energy levels introduced by this highly inhomogeneous chirped QD system result in thermal broadening of carrier population in energy. Refer to chirpily stacked QD laser structure Section II-D, the emissions wavelengths for ES of $2^{*}\mathrm{QD_L}$ (1.19 μm), GS of $3^{*}\mathrm{QD_M}$ (1.22 μm), and GS of $5^{*}\mathrm{QD_S}$ (1.17 μm) are indeed within the thermal broadening energy range of 25.6 meV.

Also, as shown in Fig. 6(b), the slope illustrated by dotted lines is steeper for long cavity devices. It is consistent with the fact that excess carrier leakage is much reduced under lower injected current densities. By fitting the data points of 1500 μm cavity to (10), $dg/dn = 2.4 \times 10^{-15}$ cm^2 with reduced $\varepsilon = 3 \times 10^{-15}$ cm^3 is then achieved.

IV. Conclusion

In summary, we have investigated the dynamic properties of InAs–InGaAs–GaAs QD lasers by the parasitic-free RIN measurement. The RIN spectra of GS and ES lasing emissions are measured and analyzed for uniformly and chirpily stacked multilayer QD lasers, respectively. Analysis of resonance frequency versus damping coefficient as well as incremental current resolves the dynamic parameters of K-factor and D-factor, where device parameters of maximum bandwidth, differential gain, and gain compression factor are extracted within.

For uniformly stacked QD lasers of GS lasing emission at 1.3 μm range, the K-factor limited bandwidth is as high as 13 GHz. The extracted differential gain and gain compression factor are 1.7×10^{-15} cm^2 and 2×10^{-16} cm^3, respectively. While for chirpily stacked QD lasers of ES lasing emission at 1.2 μm range, the K-factor limited bandwidth is 14 GHz. Yet the linear, instead of proportional, dependence between resonance frequency and square root of incremental current is observed and attributed to the huge gain compression associated with excess carrier leakage in the highly inhomogeneous chirpily stacked QD system. The extracted differential gain and gain compression factor for ES lasing emissions are 4.3×10^{-15} cm^2 and 1.4×10^{-14} cm^3, respectively.

Acknowledgment

The authors are grateful to K. F. Lin of Industrial Technology Research Institute for device fabrication. The MBE growth of QD laser structures was credited to Innolume GmbH, Dortmund, Germany.

References

[1] K. Otsubo, N. Hatori, M. Ishida, S. Okumura, T. Akiyama, Y. Nakata, H. Ebe, M. Sugawara, and Y. Arakawa, "Temperature-insensitive eye-opening under 10-Gb/s modulation of 1.3-μm p-doped quantum-dot lasers without current adjustments," *Jpn. J. Appl. Phys.*, vol. 43, pp. L1124–L1126, 2004.

[2] S. Fathpour, Z. Mi, and P. Bhattacharya, "High-speed quantum dot lasers," *J. Phys. D*, vol. 38, pp. 2103–2111, 2005.

[3] B. J. Stevens, D. T. D. Childs, H. Shahid, and R. A. Hogg, "Direct modulation of excited state quantum dot lasers," *Appl. Phys. Lett.*, vol. 95, p. 061101, 2009.

[4] K. Takada, Y. Tanaka, T. Matsumoto, M. Ekawa, H. Z. Song, Y. Nakata, M. Yamaguchi, K. Nishi, T. Yamamoto, M. Sugawara, and Y. Arakawa, "Wide temperature-range 10.3 Gbit/s operations of 1.3 μm high-density quantum-dot DFB lasers," *Electron. Lett.*, vol. 47, pp. 206–208, 2011.

[5] M. Ishida, Y. Tanaka, K. Takada, T. Yamamoto, H. Z. Song, Y. Nakata, M. Yamaguchi, K. Nishi, M. Sugawara, and Y. Arakawa, "Effect of carrier transport on modulation bandwidth of 1.3-μm InAs–GaAs self-assembled quantum-dot lasers," in *Proc. 22th IEEE Int. Semicond. Laser Conf.*, 2010, pp. 174–175.

[6] P. Resneau, M. Calligaro, S. Bansropun, O. Parillaud, M. Krakowski, R. Schwertberger, A. Somers, J. P. Reithmaier, and A. Forchel, "High power, very low noise and long term ageing 1.55 μm InP-based Fabry-Perot quantum dash lasers under CW operation," in *Conf. Lasers Electro-Opt.*, 2005, pp. 1805–1807.

[7] M. Krakowski, P. Renseau, M. Calligaro, H. Liu, and M. Hopkinson, "High power, very low noise, CW operation of 1.32 μm quantum-dot Fabry-Perot laser diodes," presented at the presented at the 20th IEEE Int. Semicond. Laser Conf., Kohala Coast, HI, Paper TuC4.

[8] A. Capua, L. Rozenfeld, V. Mikhelashvili, G. Eisenstein, M. Kuntz, M. Laemmlin, and D. Bimberg, “Direct correlation between a highly damped modulation response and ultra low relative intensity noise in an InAs–GaAs quantum dot laser,” *Opt. Exp.*, vol. 15, pp. 5388–5393, 2007.

[9] A. Martinez, K. Merghem, S. Bouchoule, G. Moreau, A. Ramdane, J.-G. Provost, F. Alexandre, F. Grillot, O. Dehaese, R. Piron, and S. Loualiche, “Dynamic properties of InAs–InP (311)B quantum dot Fabry-Perot lasers emitting at 1.52 μm,” *Appl. Phys. Lett.*, vol. 93, p. 021101, 2008.

[10] M. C. Tatham, I. F. Lealman, C. P. Seltzer, L. D. Westbrook, and D. M. Cooper, “Resonance frequency, damping, and differential gain in 1.5 μm multiple quantum-well Lasers,” *IEEE J. Quantum Electron.*, vol. 28, no. 2, pp. 408–414, Feb 1992.

[11] N. Yokouchi, N. Yamanaka, N. Iwai, Y. Nakahira, and A. Kasukawa, “Tensile-strained GaInAsP-InP quantum-well lasers emitting at 1.3 μm,” *IEEE J. Quantum Electron.*, vol. 32, no. 12, pp. 2148–2155, Dec. 1996.

[12] R. Nagarajan, M. Ishikawa, T. Fukushima, R. S. Geels, and J. E. Bowers, “High speed quantum-well lasers and carrier transport effects,” *IEEE J. Quantum Electron.*, vol. 28, no. 10, pp. 1990–2008, Oct. 1992.

[13] T. Keating, X. Jin, S. L. Chuang, and K. Hess, “Temperature dependence of electrical and optical modulation responses of quantum-well lasers,” *IEEE J. Quantum Electron.*, vol. 35, no. 10, pp. 1526–1534, Oct. 1999.

[14] M. Ishida, N. Hatori, T. Akiyama, K. Otsubo, Y. Nakata, H. Shoji, H. Ebe, M. Sugawara, and Y. Arakawa, “Photon lifetime dependence of modulation efficiency and K factor in 1.3 μm self-assembled InAs–GaAs quantum-dot lasers: Impact of capture time and maximum modal gain on modulation bandwidth,” *Appl. Phys. Lett.*, vol. 85, pp. 4145–4147, 2004.

[15] H. Su and L. F. Lester, “Dynamic properties of quantum dot DFB lasers: High speed, linewidth and chirp,” *J. Phys. D*, vol. 38, pp. 2112–2118, 2005.

[16] M. Gioannini, A. Sevega, and I. Montrosset, “Simulations of differential gain and linewidth enhancement factor of quantum dot semiconductor lasers,” *Opt. Quantum. Electron.*, vol. 38, pp. 381–394, 2006.

[17] A. H. Al-Khursan, “Intensity noise characteristics in quantum-dot lasers: Four-level rate equations analysis,” *J. Lumin.*, vol. 113, pp. 129–136, 2005.

[18] A. Fiore and A. Markus, “Differential gain and gain compression in quantum-dot lasers,” *IEEE J. Quantum Electron.*, vol. 43, no. 4, pp. 287–294, Apr. 2007.

[19] G. Lin, C. Y. Chang, W. C. Tseng, C. P. Lee, K. F. Lin, R. Xuan, and J. Y. Chi, “Novel chirped multilayer quantum-dot lasers,” in *Proc. SPIE*, 2008, vol. 6997, p. 69970R.

[20] H. Lu, C. Blaauw, B. Benyon, G. P. Li, and T. Makino, “High-power and high-speed performance of 1.3-μm strained MQW gain-coupled DFB lasers,” *IEEE J. Sel. Topics Quantum Electron.*, vol. 1, no. 2, pp. 375–380, Jun. 1995.

[21] T. Fukushima, R. Nagarajan, M. Ishikawa, and J. E. Bowers, “High-speed dynamics in InP based multiple quantum well lasers,” *Jpn. J. Appl. Phys.*, vol. 32, pp. 70–83, 1993.

[22] J. E. Bowers and M. A. Pollack, “Semiconductor lasers for telecommunications,” in *Optical Fiber Telecommnications II*, S. E. Miller and I. P. Kaminow, Eds. New York: Academic, 1988, pp. 509–568.

[23] D. Klotzkin and P. Bhattacharya, “Temperature dependence of dynamic and DC characteristics of quantum-well and quantum-dot lasers: A comparative study,” *J. Lightw. Technol.*, vol. 17, no. 9, pp. 1634–1641, Sep. 1999.

[24] P. Bhattacharya, S. Ghosh, S. Pradhan, J. Singh, Z. K. Wu, J. Urayama, K. Kim, and T. B. Norris, “Carrier dynamics and high-speed modulation properties of tunnel junction InGaAs-GaAs quantum-dot lasers,” *IEEE J. Quantum Electron.*, vol. 39, no. 8, pp. 952–962, Aug. 2003.

[25] M. Sugawara, K. Mukai, and H. Shoji, “Effect of phonon bottleneck on quantum-dot laser performance,” *Appl. Phys. Lett.*, vol. 71, pp. 2791–2793, 1997.

[26] F. Grillot, B. Dagens, J. G. Provost, H. Su, and L. F. Lester, “Gain compression and above-threshold linewidth enhancement factor in 1.3-μm InAs-GaAs quantum-dot lasers,” *IEEE J. Quantum Electron.*, vol. 44, no. 10, pp. 946–951, Oct. 2008.

Gray Lin (M’08) was born in Miaoli, Taiwan, in 1972. He received the B.S., M.S. and Ph.D. degrees from the Department of Electronics Engineering and Institute of Electronics, National Chiao-Tung University, Hsinchu, Taiwan, in 1994, 1995, and 2001, respectively. His doctoral research dealt with semiconductor lasers with quantum structure, both quantum wells and quantum dots.

From 2001 to 2007, he was with the Opto-Electronics and Systems Laboratories, Industrial Technology Research Institute, Hsinchu, where he carried on the substitute military service. Since February 2007, he has been a Faculty Member in the Department of Electronics Engineering and Institute of Electronics, National Chiao-Tung University. His research interests include molecular beam epitaxy growth of GaAs-based compound semiconductor materials, design and fabrication of semiconductor lasers, as well as characterization and analysis of opto-electronic devices.

Hao-Ling Tang, biography not available at the time of publication.

Hsu-Chieh Cheng, biography not available at the time of publication.

Hung-Lin Chen, biography not available at the time of publication.